We are IntechOpen, the world's leading publisher of Open Access books
Built by scientists, for scientists

6,900
Open access books available

186,000
International authors and editors

200M
Downloads

Our authors are among the

154
Countries delivered to

TOP 1%
most cited scientists

12.2%
Contributors from top 500 universities

CLARIVATE ANALYTICS
BOOK CITATION INDEX
INDEXED

WEB OF SCIENCE™

Selection of our books indexed in the Book Citation Index
in Web of Science™ Core Collection (BKCI)

Interested in publishing with us?
Contact book.department@intechopen.com

Numbers displayed above are based on latest data collected.
For more information visit www.intechopen.com

Localizing with Passive UHF RFID Tags Using Wideband Signals

Andreas Loeffler and Heinz Gerhaeuser

Additional information is available at the end of the chapter

1. Introduction

Localization of positions and detection of objects is a key aspect in today's applications and, although the topic exists a while ago, it is still under ongoing research. The introduction of global navigation satellite systems (GNSS), particularly GPS [1], and its improvements with accuracies down to a few meters, was a huge step towards ubiquitous localization [2, 3]. This is almost valid for outdoor environments, whereas indoor localization is still a challenging issue [4, 5]. The reason for that is the demanding, dynamic indoor environment, causing severe multipath fading, leading to hard predictable propagation models - thus influencing time, power and phase measurements. However, in the past, much effort has been put into designing high accurate indoor localization systems, including technologies like ultrasonic sound, infrared light, Wi-Fi, Bluetooth, ZigBee, cellular mobile communication (GSM, UMTS), ultra-wideband and RFID just to mention a few of them. Despite all the effort, there is no outstanding technology comprising all indoor localization contingencies as every technology in use has its advantages and disadvantages regarding accuracy, availability, complexity and costs.

Due to constantly falling prices of UHF RFID tags [6] additional applications arose beside the traditional concept of radio frequency identification (RFID). Major applications include supply chain technologies [7] and logistics [8], from container level tagging even down to item level tagging [9]. Regarding the Internet of Things [10], UHF RFID has some advantages over other RFID technologies, i.e., LF and HF: UHF RFID tags are small, do not require a battery, allow high data rates and high reading ranges, whereas LF and HF cannot serve with these issues at the same time [10]. Together with the mentioned low costs, the UHF RFID technology may be available in lots of objects (walls, carpets, doors, etc.) in the future. Therefore, indoor positioning using UHF RFID technology could be one solution towards ubiquitous localization, as efforts are made to shrink the size of RFID reader ICs and to integrate them into mobile phones.

The chapter is organized as follows. Section 2 gives a brief overview of today's wireless positioning technologies with a focus on RFID. Section 3 introduces the proposed positioning system and shows the theoretical approach along with an example. Section 4 focuses on challenges and limitations of the system and Section 5 presents results from measurements carried out underlining the principle of operation. Section 6 provides a discussion based on the results. Finally, Section 7 gives a short summary and concludes with a perspective for future work.

2. Basics and state of the art

This section provides an overview of state-of-the-art wireless positioning technologies. The section is divided into two subsections, with the first subsection describing measurement principles for positioning, whereas the second subsection has a focus on current positioning technologies based on RFID, particularly UHF RFID within the 900 MHz frequency band.

2.1. Positioning measurement principles

The first paragraph provides definitions for the terms precision, rightness and accuracy, whereas the following paragraphs describe the main positioning processes comprising lateration, angulation and fingerprinting. The last paragraph depicts the measurement techniques used for the positioning process, for instance, time of arrival, angle of arrival and received signal strength.

2.1.1. Precision, rightness and accuracy

Often, the terms "precision" and "accuracy" are used to define the same issue, namely how well a localization system or method works, e.g., the measurement error expressed in meters. However, precision and accuracy are not similar to each other. Therefore, this paragraph points out the differences and relations of the terms precision, rightness and accuracy.

Precision shows how well independent measurement values are located to each other. That means, if many measurement values are in dense proximity to each other, the measurement has a high precision; on the other hand, it does not mean that the measurement is accurate in any case. A standard term that is used to measure the precision is the standard deviation σ_x with

$$\sigma_x = \sqrt{E\left\{\left(\hat{x} - E\{\hat{x}\}\right)^2\right\}} \text{ and } \hat{\sigma}_x = \sqrt{\frac{1}{N-1}\sum_{k=1}^{N}\left(\hat{x}_k - \bar{\hat{x}}\right)^2}, \text{ with} \tag{1}$$

$$\bar{\hat{x}} = \frac{1}{N}\sum_{k=1}^{N}\hat{x}_k \tag{2}$$

$\hat{\sigma}_x$ describes the estimated standard deviation of the measurement, N describes the number of measurements, $\hat{x}_k$ the measurement value at the kth measurement, $\bar{\hat{x}}$ the estimated mean

value of the measurement values. $\hat{x}$ describes the random variable of the measurement process, whereas $E\{\cdot\}$ is the corresponding expectation value. In the following, the standard deviation σ_x is used as a measure for the precision of a positioning technique.

Rightness or trueness describes how well the measured values respectively the expectation of the estimated values $\hat{x}$ fit to the expectation of the true values x, i.e., a so called bias with

$$Bias = E\{\hat{x} - x\} = E\{\hat{x}\} - x \quad \text{and} \quad \widehat{Bias} = \bar{\hat{x}} - \bar{x} \tag{3}$$

$\widehat{Bias}$ is the estimated rightness of the measurement and $\bar{x}$ is the mean value of the true values. The rightness is a measure for the average discrepancy between a measured and a reference value and may be described as bias or offset.

Accuracy takes both, the precision and the rightness, into account. In fact, only high accuracy may be achieved if precision and rightness is high, too. A well known definition of the accuracy is the root mean square error RMSE, which is defined as

$$\text{RMSE}=\sqrt{\text{MSE}}=\sqrt{E\{(\hat{x} - x)^2\}} \quad \text{and} \quad \widehat{\text{RMSE}}=\sqrt{\frac{1}{N}\sum_{k=1}^{N}(\hat{x}_k - x_k)^2} \tag{4}$$

$\widehat{\text{RMSE}}$ describes the estimated RMSE of the measurement and x_k the true value at the the kth measurement.

According to [11] the first expression in Equation (4) can be transformed into

$$\text{RMSE}=\sqrt{\sigma_x^2 + \text{Bias}^2} \tag{5}$$

Equation (5) shows that a distorted measurement with a high precision may be more accurate than an undistorted measurement with a low precision respectively standard deviation.
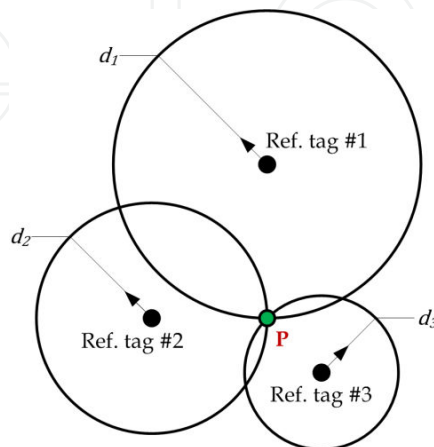

Figure 1. Example of trilateration with RFID reference tags

2.1.2. Lateration

Lateration is used to determine the position using distances to known reference points. For instance, an RFID reader may localize itself by evaluating distances to certain reference points, e.g., RFID tags, using the principle of trilateration, as shown in Figure 1. In this figure, two-dimensional (2D) positioning of **P**, an RFID reader, can be realized using three reference points, here reference tags. Assuming the reader is able to exactly determine its distance $d_i \; \forall \, i \in \{1,2,\, 3\}$ to each of the tags, a circle is drawn around each tag with radius equal to the measured distance d_i. The intercept point of the three circles with radii $d_1 \ldots d_3$ indicates the position of the reader **P**. If the positions of the reference tags are known, the reader may determine its position by solving the set of equations

$$\sqrt{(x_P - x_i)^2 + (y_P - y_i)^2} = d_i, \quad i \in \{1,2,\, 3\}. \tag{6}$$

$(x_P; y_P)$ is the position of the reader, which shall be estimated and $(x_i; y_i) \; \forall \, i \in \{1,2,\, 3\}$ is the position of each of the reference points respectively tags. Solving the set of equations in (6) for three reference points yields [12, 13]:

$$\begin{pmatrix} x_P \\ y_P \end{pmatrix} = \begin{pmatrix} a_{1,2} & b_{1,2} \\ a_{1,3} & b_{1,3} \end{pmatrix}^{-1} \begin{pmatrix} g_{1,2} \\ g_{1,3} \end{pmatrix}, \tag{7}$$

with

$$a_{1,i} = 2(x_i - x_1), \quad i \in \{2,3\} \tag{8}$$

$$b_{1,i} = 2(y_i - y_1), \quad i \in \{2,3\} \tag{9}$$

and

$$g_{1,i} = d_1^2 - d_i^2 - (x_1^2 + y_1^2) - (x_i^2 + y_i^2), \quad i \in \{2,3\}. \tag{10}$$

In the case of three-dimensional (3D) positioning, a minimum of four reference points is necessary to unambiguously determine the exact position. However, due to the imperfectness of the distance measurement (noise, fading channel, etc.), there is usually no exact interception point, but rather an intersection area. Therefore, different error-minimizing algorithms can be used to make a best estimate for the position determination [14]. The accuracy of the measurements can be further increased by making use of more than the necessary minimum of reference points [15].

In RFID, generally, there exists clock synchronization between transmitter and receiver, as both components are located within the RFID reader. If, however, there is no clock synchro-

nization between transmitter and receiver, the clock offset τ_{offset} will lead to a constant distance error d_{offset} within each range measurement. This additional parameter can be solved by adding one more equation (equal to one additional tag) to the minimum number of equations when there is no synchronization error:

$$\sqrt{(x_P - x_i)^2 + (y_P - y_i)^2} + d_{\text{offset}} = d_i \quad \forall \, i \in \{1,2,\, 3,4\} \tag{11}$$

As mentioned before, there should be no time offset in RFID systems. Nevertheless, constant phase shifts due to the non-constant reflection coefficient of RFID tags [16] can lead to an additional offset distance d_{offset}, having the same effect as a time-based clock offset. The set of equations in (11) describe hyperbolas rather than circles around the reference points. Figure 2 shows the effect of an offset distance d_{offset} and two out of four hyperbolic curves, which would intercept in position P.
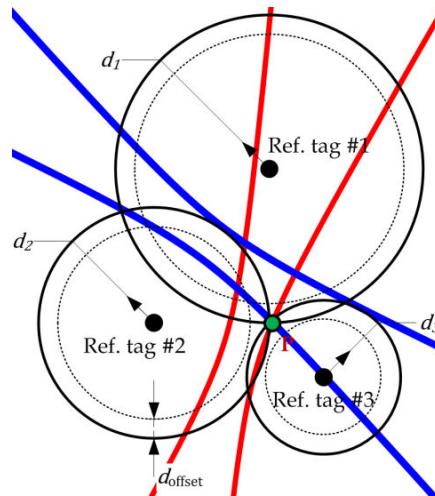

Figure 2. Example of hyperbolic lateration using RFID tags as reference points

2.1.3. Angulation

The principle of angulation rests upon the relations between angles and distances within a triangle; therefore, it is mostly common under the term triangulation. If two angles and one side of a triangle are known the remaining distances respectively the position to be determined can be calculated using the *law of sines* and the *angle sum of a triangle*. Figure 3 shows the principle used: Two antennas (Ant. #1 and Ant. #2) of an RFID reader are deployed to calculate the position of the RFID tag. This can be realized using, for instance, phase-based or direction-defined measurements. From independent angle measurements one obtains the angles α and β; the distance d_0 is known in advance. Subsequently, the remaining angle γ is calculated (angle sum in triangle) and from that the missing two distances d_1 and d_2 from the antennas to the RFID tag (law of sines). Angulation may be used in 2D or 3D localization problems.
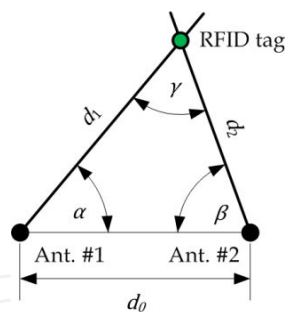
Figure 3. Triangulation example using two antennas to determine the position of an RFID tag

2.1.4. Scene-based localization / fingerprinting

Scene-based localization is divided in two sequential processes, a calibration process and an operational process. The calibration process records any environmental values (optical, electrical, physical, etc.), also known as fingerprints, at several positions within a scene and stores the data in a database [17, 18]. The following operational process is thus able to determine the position by measuring the current environmental values and comparing them with the values in the database. Special algorithms estimate the position by finding the position with the minimal error [19]. Figure 4 shows a room map with different WLAN base stations showing the electrical field strength at different locations [20] used along with WLAN positioning.
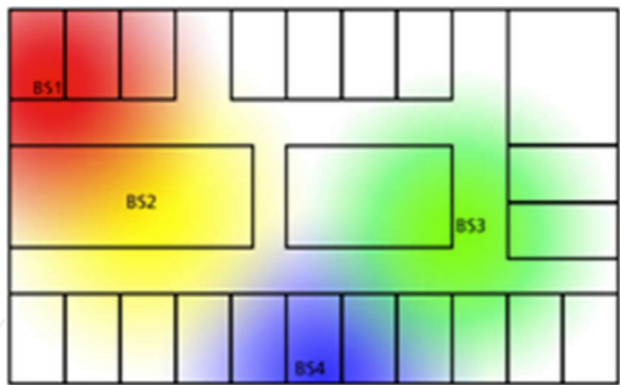

Figure 4. Electrical field strength distribution within a building to be used for WLAN positioning [20]

2.1.5. Positioning measurement techniques

After highlighting the measurement principles, this paragraph gives a brief overview over the common technologies used. Distance measurements may be based on measuring the time of flight, the signal strength and the phase between transmitted and received signal.

Time measurements include Time of Arrival (ToA) and Time Difference of Arrival (TDoA) measurements.

ToA measurements directly determine the distance by using the time of flight t_{ToA} of the signal. Multiplied with the corresponding propagation speed c, the speed of light in case of electro-magnetic waves, this results directly in the distance d_{ToA} between transmitter and receiver as described in Equation (12). ToA measurements can be used directly along with trilateration methods.

$$d_{\text{ToA}} = t_{\text{ToA}} \cdot c \qquad (12)$$

TDoA measurements determine the time difference of a signal received at known reference points rather than measuring directly the time between transmitter and receiver. This means, that the time stamp of the signal transmitted via the object to be localized is unknown, but the time differences at the synchronized receivers are determined. In contrast to ToA, TDoA does not require any synchronization between transmitter and receiver. The reference stations must be synchronized, indeed. One positioning method using TDoA measurements is hyperbolic lateration (see Paragraph 2.1.2).

RSS (Received Signal Strength) measurements are based on the received signal strength at the receiver. Hence, there are two possible candidates to process RSS-based data. The first one is based on the propagation conditions, usually including a modified and enhanced form of Friis transmission equation

$$P_r = P_t + G_t + G_r + 20 \log\left(\tfrac{\lambda}{4\pi d}\right) [\text{dB}], \qquad (13)$$

e.g., the log-distance path loss model

$$\text{PL}(d) = \text{PL}(d_0) + 10\alpha \log\left(\tfrac{d}{d_0}\right) + X \ [\text{dB}]. \qquad (14)$$

Equation (13) describes the free space attenuation formula depending on the distance d and wavelength λ with receiving power P_r, transmitting power P_t, receiving and transmitting antenna gains G_t and G_r together with the free space attenuation $\left(\tfrac{\lambda}{4\pi d}\right)^2$ in dB. Equation (14) on the other hand describes the path loss $\text{PL}(d)$ depending on the distance d related to a reference path loss $\text{PL}(d_0)$ at distance d_0. The path loss may be described as the difference of transmitted and received power in dB. α represents the path loss exponent that depends on the propagation environment, whereas X is a zero-mean Gaussian distributed random variable describing the fading effects at different locations and instants of time. If, in case of the usage of Equation (14), $\text{PL}(d_0)$, α and the variance of X is known, one can calculate directly the probability for a certain distance d between transmitter and receiver. One disadvantage is that α and X are very dependent on the environment and can change significantly. The RSS measurements can be used along with lateration methods.

The second RSS-based approach is to measure in advance RSS values at certain positions within the localization area (fingerprints). The measured values are pre-processed and stored into a database. During the proper localization process, the current measurement values are compared to the values in the database and a best-fit position, based on the current values, is estimated. The advantage of using RSS values for this approach is that almost all devices come along with some kind of RSS-based output, including RFID readers. This method is used in scene-based positioning techniques.

Phase measurements can be used to provide information about speed, distance and angle. A good overview over these techniques is given in [21]. The radial velocity v of a tag is measured by evaluating the phase shift $\partial\varphi$ during different moments in time ∂t as given in Equation (15).

$$v = - \frac{c}{2\omega_0} \frac{\partial\varphi}{\partial t} \tag{15}$$

with c being the propagation speed and ω_0 the fixed circular frequency. The distance d between a tag and a reader can be calculated according to Equation (16) by measuring the phase shift at different frequencies.

$$d = - \frac{c}{4\pi} \frac{\partial\varphi}{\partial f} \tag{16}$$

Finally, phase measurements may be used to measure the angle θ between reader and tag (Angle of Arrival, AoA) using multiple receiving antennas. For two receiving antennas, Equation (17) describes the relation between the incoming angle θ, the phase difference $\varphi_2 - \varphi_1$ at a certain carrier frequency, and the spacing a between the receiving antennas.

$$\theta \approx \sin^{-1}\left[-\frac{c}{\omega} \frac{\varphi_2 - \varphi_1}{a}\right] \tag{17}$$

Phase measurement are used along with lateration and angulation principles to calculate the distance between transmitter and receiver respectively reader and tag.

2.2. Survey on UHF RFID-based localization systems

The following paragraphs provide a brief survey on state-of-the-art RFID localization systems within the UHF and microwave frequency band. The survey includes systems using RSS values, ToA and TDoA measurements, phase-based measurements as well as fingerprinting methods. Further surveys are provided in [22, 23, 24].

2.2.1. RSS-based direct range estimation

The SpotON system [25] is based on active RFID tags (working at 916.5 MHz) and provides a 3D ad hoc localization. RFID readers measure the signal strength of active RFID tags and a central server performs the calculation of the position within the environment. The relation

between the RSS value and the position is based on the indoor channel model from Seidel and Rappaport [26]. The accuracy of the SpotON system is given with a cube of 3 m edge length, but this is dependent on the number of reference tags used. A disadvantage of the system is the long position calculation time from 10 to 20 s; an advantage is the easy to extend infrastructure and low system costs.

2.2.2. ToA-based range estimation

A 2.4 GHz RFID system based on SAW transponders is described in [27]. The SAW tags use a bandwidth of 40 MHz and reduce the echoes from the environment as the reflected tag signal is delayed due to the lower surface speed on the SAW material. The signal time on the SAW transponder is T_{SAW}=2.2 μs; so the reflections and echoes from the reader are almost faded out before the SAW-reflected signal responses back to the reader. A three-antenna system is used to perform a 2D positioning. However, the localization accuracy is strongly temperature-dependent and adds up to around 20 cm in a room with the dimension 2 m × 2 m.

2.2.3. TDoA-based range estimation

A localization system in the 5.8 GHz frequency band is described in [28]. The system is build upon active transponders and multiple base stations. One reference transponder is used as wireless synchronization source for the base stations. The system operates on the FMCW (frequency modulated continuous wave) principle (see [29]) and evaluates the time difference of a measurement transponder signal to determine the position of the measurement transponder. The position accuracy is given with 10 cm on an area of 500 m × 500 m.

2.2.4. Phase-based range estimation

The principle of FMCW is used to measure the distance to a certain object. The idea behind FMCW is to sweep a frequency band with the sweep rate α and record the phase and frequency differences. Furthermore, the transmitted signal from the reader is modulated by the transponder with a modulation frequency f_{mod}. The usage of a modulation frequency shifts the measurement signal into a higher frequency band (by f_{mod}), in order to suppress certain disturbances and noise within the baseband. The distance d is calculated through the frequency difference Δf and the phase difference $\Delta \varphi$ [30], with the latter providing a high range resolution within half a wavelength of the signal. Therefore, Δf provides a coarse distance estimation and $\Delta \varphi$ a more accurate one. $\Delta \varphi$ alone cannot be used as direct distance estimation due to ambiguities of the phase information. According to [30] the distance to a transponder can be calculated with

$$d_{coarse} = \frac{\pi \cdot c \cdot \Delta f}{2 \cdot \alpha} \text{ and } d_{precise} = \frac{c \cdot \Delta \varphi}{4 \cdot \omega_0}. \tag{18}$$

[31] describes an FMCW-based RFID system using a transponder with an UHF front-end working at 868 MHz. The transponder IC provides a modulation frequency of

f_{mod}=300 kHz and is driven by a 2.45 GHz FMCW signal with a bandwidth of 75 MHz. The system is tested on a cable-based setup and delivers an RMSE of 1 cm with cable lengths between 1 m and 9.5 m.

The system in [32] uses the phase difference observed at different frequencies to estimate the range between transponder and reader. The range estimation is performed according to Equation (16), whereas the maximum range d_{max} due to phase ambiguities is given with

$$d_{max} = \frac{c}{2B}. \qquad (19)$$

However, the choice of the bandwidth B strongly influences the system's capabilities. A high B generates a high accuracy but a low maximum range; a low B leads to a higher range but at the expenses of a lower accuracy. Simulations at an SNR of 10 dB results in errors of 2.5 m for a frequency separation of B=1 MHz, and errors of 0.1 m for a B of 26 MHz. One has to keep in mind that the separation of 26 MHz is only valid within the US frequency band for RFID that ranges from around 902 MHz to 928 MHz. The European band is smaller (865.6 MHz to 867.6 MHz) leading to a lower accuracy.

2.2.5. Scene-based range estimation

LANDMARC [33] is an extension and improvement of the SpotON system [25, 34]. The system consists of fixed RFID readers, active reference tags (landmarks) and tags to be localized. The system uses RSS values connected with the kNN (k-nearest neighbor) algorithm [35] to estimate the position. The average error of the system is given with 1 m [33].

[36] examines the localization error of the LANDMARC system using passive, instead of active RFID tags. As a result, the orientation of the tags has a major influence on the total performance of the system. Using the kNN algorithm, in 47.5 % of the cases, the error was less than 0.5 m and in 27.5 % of the cases, the error was less than 0.3 m. However, in comparison to the original LANDMARC system, the overall range is smaller due to the usage of passive RFID technology.

A system based on a particle filter is proposed in [37]. It uses two RFID readers mounted on a small mobile vehicle to localize itself using RSS values. The calibration phase is performed in a room of size 5 m × 10 m. Depending on the speed of the vehicle and the material on which the tags are located (plastics, concrete, metal) the average error is between 1.35 cm and 2.48 cm. This system is based on the mobile robot system in [38] that incorporates a SLAM algorithm [39] based on Monte Carlo methods [40].

[41] describes a positioning system using fingerprints (RSS values and read rate) to localize tagged objects. First, a rough positioning is done using antenna cells, with each antenna illuminating a different room zone. This rough classification is realized using either Bayesian filter, kernel density estimation (KDE) based measurement models, support vector machines (SVM) or LogitBoost [42]. RSS-based values and read rate is used along with the algorithms to roughly estimate the position of the tagged object. One result was that the estimations based on RSS values perform better than the estimations based on the read rate. An even more

accurate positioning is realized when RSS values are used along with read rates of the transponders. Within the calibration phase, one tries to generate a high amount of reference points (fingerprints). Two algorithms are used and compared to perform within the positioning phase, a cascaded algorithm and a kNN algorithm. The cascaded algorithm runs the rough localization followed by the kNN algorithm for the high accuracy. The second algorithm resigns to use the rough position estimation. Similarly, the RSS-based fingerprints perform better than the read rates. Dependent on the environment, positioning errors between 37.9 cm and 42.1 cm may be achieved.

3. Wideband UHF RFID positioning system

This section introduces a brief motivation for the realized RFID positioning system before describing the basic structure of the system.

As derived from Section 2, current passive RFID localization systems suffer either from a high effort in the calibration phase (fingerprinting) or from bandwidth limitations which hold down the system's overall accuracy. Higher accuracies may be achieved using phase-based approaches at the expense of more complex hardware structures and necessary volume (see, for instance, phased array antennas [43]), only usable for fixed reader hardware. Therefore, an ideal passive mobile RFID positioning system should have:

• no change in hardware,

• high bandwidth,

• direct position estimation.

The here proposed system offers high bandwidth, but with very low power, and is based on a ToA method performing direct position estimation. As a consequence, additional hardware effort is necessary to provide the generation and evaluation of the high bandwidth signals.

In the following, a brief overview of the system, particularly its principle working structure, is provided.

Assuming a scenario as given in Figure 5. The scenario consists of n tags, whereby the distance to the ith tag has to be evaluated. The RFID reader is indicated at the bottom (only the coupler with antenna in monostatic mode) with input signal x_{reader} (into the antenna) and output signal y_{reader} (from the antenna). s_1 to s_n describe the backscatter modulation factors of the transponders, i.e., the factor with which the incoming signal from the reader is reflected with (principle of backscatter). If this factor is one, the complete signal is backscattered to the reader. Indeed, data from tag to reader is transmitted by varying this factor in time with the data to be sent [10, 44]. h_1 to h_n describe the bidirectional channel impulse responses between reader and tags. For reasons of simplification the following equations and terms are written without using the time t, although the expressions depend on it.
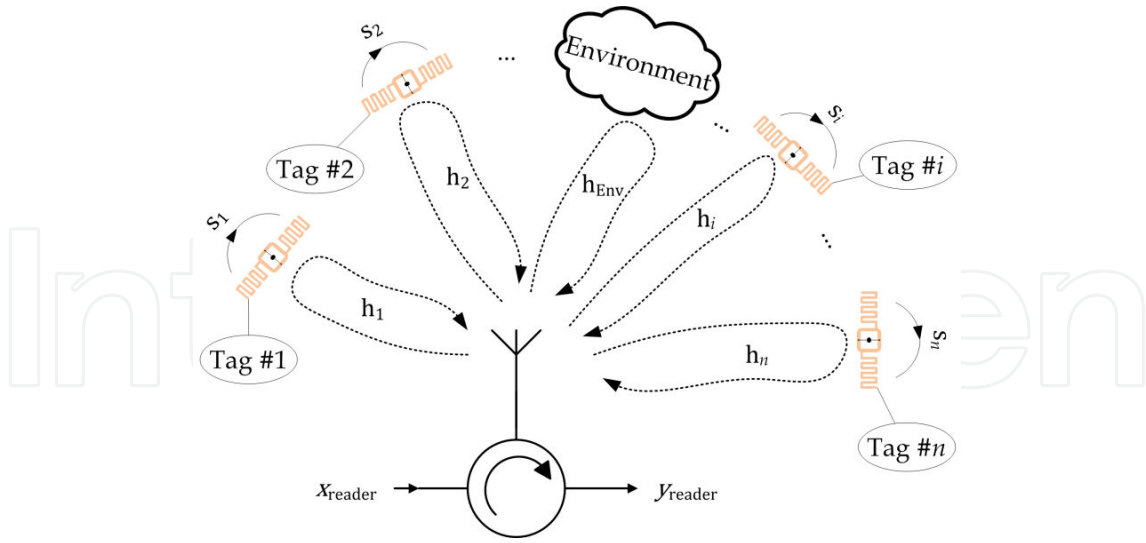
Figure 5. Scenario with passive RFID tags and reader in monostatic antenna setup

According to Figure 5 we can state (in time domain) by using the convolution $*$:

$$y_{reader} = \left[(h_1 * s_1) + (h_2 * s_2) + \dots + (h_i * s_i) + \dots + (h_n * s_n) + h_{Env} \right] * x_{reader} \qquad (20)$$

For simplicity, let us assume that each backscatter modulation factor s_i has two modulation states according to

$$s_i = \begin{cases} s_{i,1} & \text{for modulation state 1} \\ s_{i,2} & \text{for modulation state 2} \end{cases} \qquad (21)$$

In a first attempt, all tags are set into modulation state 1. The resulting signal $y_{reader,1}$ is

$$y_{reader,1} = \left[(h_1 * s_{1,1}) + (h_2 * s_{2,1}) + \dots + (h_i * s_{i,1}) + \dots + (h_n * s_{n,1}) + h_{Env} \right] * x_{reader} \qquad (22)$$

In a second attempt, only tag #*i* is set into modulation state 2, all other tags stay in modulation state 1. This can be described as one small sequence of data transmission from the *i*th tag to the reader (uplink). The resulting signal $y_{reader,2}$ is

$$y_{reader,2} = \left[(h_1 * s_{1,1}) + (h_2 * s_{2,1}) + \dots + (h_i * s_{i,2}) + \dots + (h_n * s_{n,1}) + h_{Env} \right] * x_{reader} \qquad (23)$$

The difference Δy_{reader} between both resulting signals $y_{reader,1}$ and $y_{reader,2}$ is

$$\Delta y_{reader} = y_{reader,2} - y_{reader,1} = \left[(h_i * s_{i,2}) - (h_i * s_{i,1}) \right] * x_{reader} = \left[s_{i,2} - s_{i,1} \right] * h_i * x_{reader}, \qquad (24)$$

thus, taking the difference results into observation of the ith tag with the ith channel. By assuming that the tag's data contain the position of the tag (i.e., a reference tag), the reader has to evaluate the ith channel, regarding the range, to estimate the distance between reader and ith tag. In a 2D scenario, three tags must be read to get the position data, and three channels to the tags must be evaluated in order to localize the reader itself. The principle is described in more detail in Section 4.

The experimental hardware architecture of the reader is shown in Figure 6.
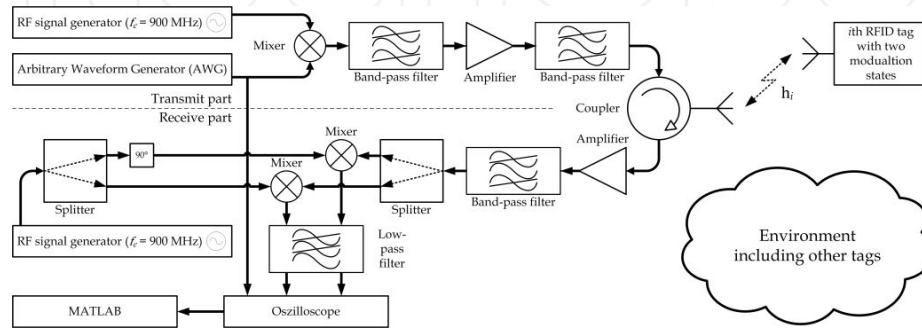

Figure 6. Experimental hardware architecture of the realized RFID localization system based on passive UHF RFID tags

The frequency-coupled RF signal generators generate carrier signals at the center frequency of f_c =900 MHz. The arbitrary waveform generator (AWG) creates the localization signal x_{reader} (in baseband). After upconversion of the localization signal, it is filtered, amplified and emitted into the environment through the antenna. The backscattered signal from the tag, the environment, and all other tags which may be in read range is also amplified, filtered and downconverted into complex baseband. The baseband signals are low-pass filtered and sampled with an oscilloscope, as is the original transmitted localization signal. Further processing is realized in MATLAB. Exemplary signals are shown in Section 6.

3.1. Derivation of the localization principle

Based on the result of the last equation (24) in Section 3, it is necessary to evaluate the channel response h_i regarding the distance between tag and reader. As stated at the beginning of Section 3 the localization should be performed using direct distance estimation, thus, the signal's time of flight t has to be evaluated in order to determine the distance d with the help of the propagation speed c, i.e.,

$$d = \frac{1}{2} c \cdot t, \tag{25}$$

with c usually being the propagation speed of electromagnetic waves complying to the speed of light. The factor one-half is introduced to compensate for the double distance the signal has to travel, i.e., from the reader to the tag and back.

In order to have a high positioning accuracy the signal must be broad regarding bandwidth, but the free spectrum for RFID, especially in Europe, is too small for that application. Therefore, higher out-of-band frequencies must be used. However, due to legal regulations, high bandwidth signals must be very low power, if applied. Ultra-wideband (UWB) signals [45] are such kind of signals and regulated by the Federal Communications Commission (FCC) and its counterparts in other regions, in order not to disturb any other in-band applications. UWB signals are defined as signals with bandwidths greater than 500 MHz or 20 % of the arithmetic mean of lower and upper cutoff frequency. The bandwidth used for the proposed system is 100 MHz due to the capability of UHF RFID tags working worldwide from around 840 MHz up to 960 MHz. Based on these conditions, although the proposed system only occupies 11 % of the arithmetic mean of the cutoff frequencies, the idea is to use low-power spreading signals for the ranging process. These signals are used to calculate the channel to a specific tag and back, thus extracting the time of flight information. As the low-power signals are hard to evaluate directly, the SNR is increased by performing coherent integration [46].

3.2. Mathematical model

Drawing up on Section 3, Equation (24), one can see that it is possible to derive the channel's impulse response upon evaluating the difference between both modulation states of the RFID transponder. Necessary for calculating the distance between tag and reader is the signal propagation time t of the up- and downlink channel. Multiplying half of t with the propagation speed results into the distance d between tag and reader (Equation (25)). As the bandwidth is limited to 100 MHz (Subsection 4.1), the pulse width is 10 ns minimum. Accordingly, a pulse width of 10 ns corresponds to a distance of around 3 m, supposing the speed of light in air is approximately 30 cm per nanosecond. Furthermore, the distance to be covered by this passive localization system is limited to the distance passive RFID tags are able to handle, which is, currently, limited to around 8 m [47]. In addition, the transmitted signal consists of more than one single pulse. These conditions lead to the fact, that the transmit signal and the receiving signal cannot be separated in time, as in ordinary RADAR applications. Another alternative is the principle of correlation, that can be used to determine the time shifted replica of the transmit pulse signal within the receiving signal [48]. The discrete correlation $R_{xy}[\tau]$ between two signals $x[t]$ and $y[t]$ is given with

$$R_{xy}[\tau] = \sum_{k=-\infty}^{+\infty} x[k] \cdot y[\tau + k] = x[t] \cdot y[t]. \tag{26}$$

The correlation term shows the time-shifted replicas of the signal $x[t]$ within the signal $y[t]$. A local maximum within the correlation term means a high correlation between $x[t]$ and $[t]$, i.e., a high linear match. The point in time of the maximum shows the time shift between $x[t]$ and $y[t]$, that is used to calculate the time between transmitted signal $x[t]$ and received signal $y[t]$.

3.3. Example

Let us derive the principle at a simplified example. Assuming the channel of the ith transponder is noise-free and multipath-free given with just

$$h_i[t] = a \cdot \delta[t - T_{\text{delay}}] \cdot e^{j\varphi_0}, \tag{27}$$

with a representing the reciprocal of the attenuation, $\delta[t - T_{\text{delay}}]$ the time delay T_{delay} of the channel with the Dirac delta function $\delta[t]$, and an initial phase shift of φ_0. Furthermore, the transponder modulation states $s_{i,1}$ and $s_{i,2}$ are given with 0 (full tag absorption) and 1 (full tag reflection). Equation (24) may now be written as

$$\Delta y_{\text{reader}}[t] = [s_{i,2} - s_{i,1}] * h_i[t] * x_{\text{reader}}[t] = [1 - 0] * a \cdot \delta[t - T_{\text{delay}}] \cdot e^{\varphi_0} * x_{\text{reader}}[t] =$$
$$= a \cdot \delta[t - T_{\text{delay}}] \cdot e^{j\varphi_0} * x_{\text{reader}}[t] \tag{28}$$

Performing the correlation to Equation (28) leads to

$$x_{\text{reader}}[t] \cdot \Delta y_{\text{reader}}[t] = x_{\text{reader}}[t] \cdot \left(a \cdot \delta[t - T_{\text{delay}}] \cdot e^{j\varphi_0} * x_{\text{reader}}[t] \right) \tag{29}$$

The convolution of $x_{\text{reader}}[t]$ with the time-shifted Dirac impulse $\delta[t - T_{\text{delay}}]$ delivers a time-shifted signal:

$$x_{\text{reader}}[t - T_{\text{delay}}] = \delta[t - T_{\text{delay}}] * x_{\text{reader}}[t] \tag{30}$$

The correlation of $x_{\text{reader}}[t - T_{\text{delay}}]$ with the original reader signal $x_{\text{reader}}[t]$ results in a time-shifted cross-correlation signal $R_{x_{\text{reader}}}[\tau - T_{\text{delay}}]$:

$$x_{\text{reader}}[t] \cdot \Delta y_{\text{reader}}[t] = a \cdot e^{j\varphi_0} \cdot R_{x_{\text{reader}}}[\tau - T_{\text{delay}}] \tag{31}$$

Performing the square of the absolute value to Equation (31), finally, leads to

$$|x_{\text{reader}}[t] \cdot \Delta y_{\text{reader}}[t]|^2 = |a|^2 \cdot |e^{j\varphi_0}|^2 \cdot |R_{x_{\text{reader}}}[\tau - T_{\text{delay}}]|^2 = |a|^2 \cdot |R_{x_{\text{reader}}}[\tau - T_{\text{delay}}]|^2 \tag{32}$$

The wanted time delay T_{delay} is evaluated by searching for the the maximum within the term $|x_{\text{reader}}[t] \cdot \Delta y_{\text{reader}}[t]|^2$:

$$T_{\text{delay}} = \underset{\tau}{\text{argmax}} \left\{ |a|^2 \cdot |R_{x_{\text{reader}}}[t - T_{\text{delay}}]|^2 \right\} \tag{33}$$

By receiving T_{delay} the distance d between reader and tag can be calculated by evaluating Equation (25) with

$$d = \frac{1}{2} \cdot c \cdot T_{\text{delay}}. \tag{34}$$

Multipath fading and receiver noise corrupt and distort the distance estimation. Gaussian noise on the low-power signals can be suppressed through coherent integration at the receiver. However, the increase in SNR due to integration is at the cost of receiving time [46]. The effect of multipath fading is more severe as it distorts the measurements in a way that is non-predictable without any a priori knowledge of the channel, which is given for a localization system working without channel prediction. The deployment of high-gain (low beam width) antennas with an electronic beam former can reduce the amount of multipath fading to an acceptable level.

4. Challenges and limitations

This section reveals the limitations and challenges of the proposed UHF RFID positioning system. Theoretical calculations show an accuracy limit at around 1 cm with the given hardware and signal limitations.

4.1. Limitations

The limitation of the system regarding the accuracy can be estimated using the Cramér-Rao Lower Bound (CRLB) [49], which defines a lower bound for an unbiased estimator $\hat{\theta}$. This means that the unbiased estimator of θ is always worse or equal to the CRLB. For an unbiased estimator $\hat{\theta}$ the standard deviation $\sigma_{\hat{\theta}}(\theta)$ is defined as [50]:

$$\sigma_{\hat{\theta}}(\theta) \geq \sqrt{\text{CRLB}_{\hat{\theta}}(\theta)} \tag{35}$$

Estimating the time-of-flight corresponds to the following CRBL definition of the standard deviation σ_x of the localization, i.e., the precision [50, 51]:

$$\sigma_x \geq \frac{c}{2\pi \cdot B_{RMS} \cdot \sqrt{2 \cdot \text{SNR}}} \tag{36}$$

c describes the propagation speed, SNR is the signal-to-noise ratio and B_{RMS} is the effective bandwidth of the signal used and is defined as

$$B_{RMS} = \int_B f^2 |S(f)|^2 \mathrm{d}f \bigg/ \int_B |S(f)|^2 \mathrm{d}f \tag{37}$$

with the Fourier transform of the signal $S(f)$ over the signal bandwidth B.

As the CRLB states in Equation (36), possible increases in precision are possible by either increasing the effective bandwidth of the signals or increasing the signal-to-noise ratio. If the given bandwidth is fixed, only an increase in SNR results in a higher measurement precision. As stated earlier, the SNR is increased by performing coherent integration. For instance, integration over $n = 10,000$ signals, results in an SNR increase of factor 10,000, but only in a precision increase of $\sqrt{10,000} = 100$. Theoretically, it is possible to increase the SNR as high as wanted, but receiver restrictions and timeouts limit the SNR to a certain level. These restrictions, mainly due to phase and quantization noise, define the limitations or the lower bounds of the localization system to a certain precision.

The applied hardware setup delivers the following SNR values for the quantization and phase noise. Thus, the receiver has an quantization error leading to an SNR of

$$\mathrm{SNR}_{\mathrm{quantization}} \approx 50 \text{ dB} = 10^5, \tag{38}$$

and phase noise leads to an SNR of

$$\mathrm{SNR}_{\mathrm{phase}} \approx 34 \text{ dB} = 2{,}512. \tag{39}$$

The total SNR is defined as

$$\frac{1}{\mathrm{SNR}} = \frac{1}{\mathrm{SNR}_{\mathrm{quantization}}} + \frac{1}{\mathrm{SNR}_{\mathrm{phase}}} + \frac{1}{\mathrm{SNR}_{\mathrm{signal}}}. \tag{40}$$

$\mathrm{SNR}_{\mathrm{signal}}$ is the power of the signal to the Gaussian noise power at the receiver. Figure 7 shows the maximum precision σ_x over certain $\mathrm{SNR}_{\mathrm{signal}}$ values and coherent integrations with a factor of n. The effective bandwidth of the signal is given with $B_{RMS} = 36.66$ MHz. The SNR values and the effective bandwidth are derived from the receiver properties and the shape of the transmit pulse. Also, the factor one-half is considered due to half of the distance from tag to reader that reduces the precision σ_x in Equation (36) by a factor of 0.5.

As from Figure 7, it is shown that the lower bound for the standard deviation is around 1 cm. By increasing the number of coherent integrations n, the bound can be shifted to the left, which means, that the lower limit of the precision is reached for a lower $\mathrm{SNR}_{\mathrm{signal}}$ value. For the proposed system, one measurement takes 1 μs, which increases to 1 s, if the coherent integration factor is $n = 1,000,000$.

4.2. Challenges

Challenges this localization system is facing are mainly:

• Multipath fading

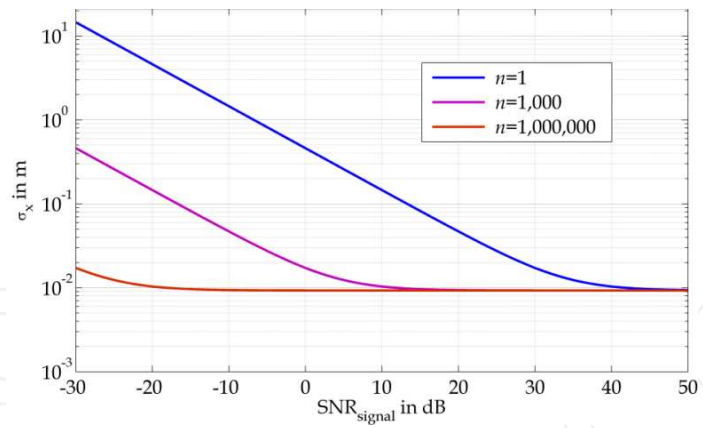• Non-constant tag reflection factors which vary by frequency and power

Figure 7. Cramér-Rao Lower Bound of the localization system
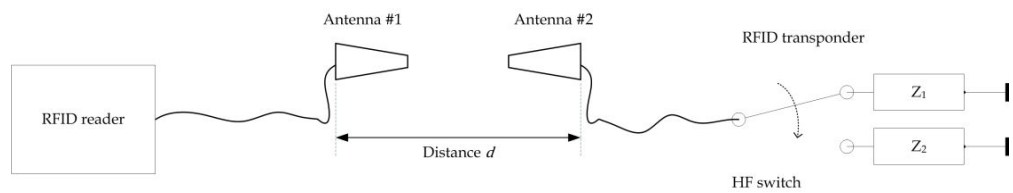

Figure 8. Measurement setup of RFID localization system

Multipath fading due to reflections, scattering and diffraction can be suppressed by using high-gain antennas with a high-focussed beam. Hence, electronic beam steering is necessary to cover the area to detect RFID tags. Using an omni-directional antenna avoids electronic beam steering at the cost of more multipath fading. Another alternative, to minimize multipath fading is the use of a much higher bandwidth. In future, UWB technology combined with RFID could have a major effect on improvements in positioning accuracy [52, 53].

The non-constant tag reflection factors that vary over frequency and power are able to strongly deteriorate the position estimation [16], if disregarded. One solution for this problem is revealed in [54].

5. Measurement results

This section shows the obtained measurement results. The first measurements are taken in an anechoic chamber, the second measurements are taken in an office environment. Both measurements are one-dimensional measurements.

5.1. Measurement setup

The measurement setup is given as in Figure 8. It consists of the reader unit as described in Section 3, an reader antenna (Antenna #1) and an RFID tag with tag antenna (Antenna #2) followed by a HF switch for emulating the tag modulation states with impedances Z_1 and Z_2. For the sake of simplicity Z_1 and Z_2 are chosen as *Short* and *Open*, i.e., $Z_1 = 0\ \Omega$ and $Z_2 = \infty\ \Omega$.
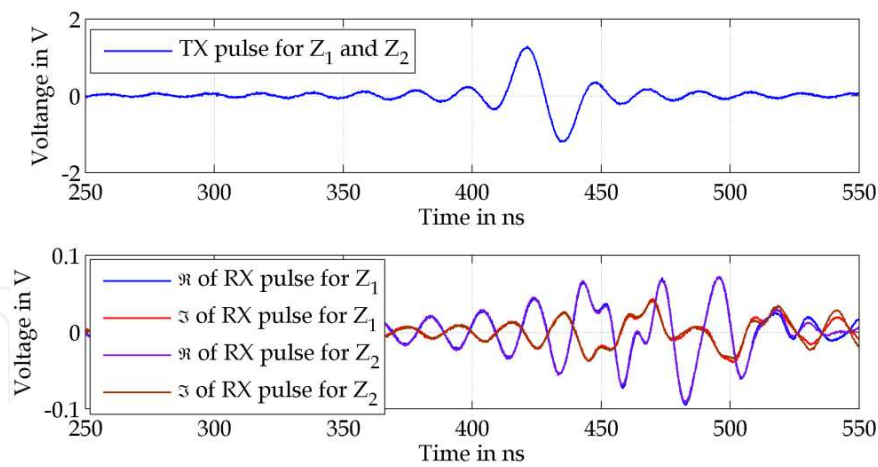
Figure 9. Exemplary transmit (TX) and receive (RX) pulses of the reader for Z_1 and Z_2, divided in real (R) and imaginary (I) signal components for an antenna to antenna distance of $d = 100$ cm

The measurement procedure is as follows. The HF switch toggles to impedance Z_1. Subsequently, the reader transmits and receives its signals as shown in Figure 9. Then, the switch toggles to Z_2 and, again, the reader transmits and receives its signals. Dependent on the number of coherent integrations, this procedure is repeated up to n. Finally, the sampled signals are evaluated in MATLAB. Figure 9 displays the transmit and receive signals for a given setup (anechoic chamber at a distance of 100 cm). The upper half of the figure shows the transmit signal – based on the Barker code [+1,-1] – used for both modulation states, Z_1 and Z_2. The lower half of the figure indicates the received signals for Z_1 and Z_2, respectively. As the received signals are complex-valued, real and imaginary parts are depicted for each RX signal. As seen in Figure 9, the received signals match each other for a certain period of time, until the difference in reflection (of Z_1 and Z_2) emerges (beginning at around 500 ns). These signals are used to determine the time shift between TX and RX signal and thus the distance between reader and tag. Evaluations of the correlations can be found in [48, 55].

The following two subsections show the measurement results, i.e., the result of the correlation difference, for two environments. First, a measurement in an anechoic chamber (Figure 10, left), second, a measurement in an office environment (Figure 10, right).
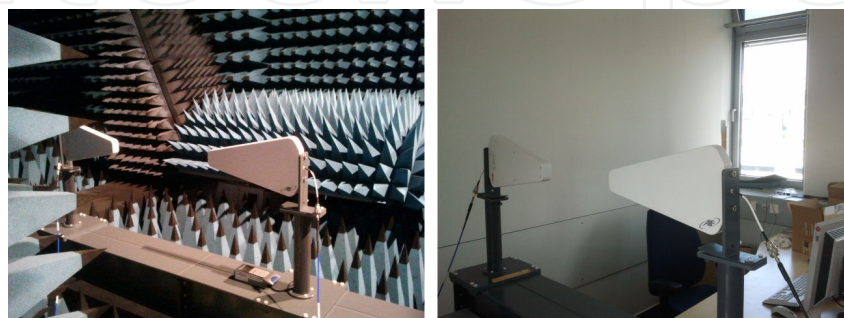

Figure 10. Measurement environments; left: anechoic chamber, right: office

5.2. Anechoic chamber measurements

The results of the measurement carried out in an anechoic chamber are depicted in Figure 11. The x-axis describes the real distances between the antennas, the y-axis describes the estimated distances. For normalization (cables, amplifiers, etc.) issues, the system is range-normalized to a distance of $d = 90$ cm (measurement with lowest variance). The coherent integration factor was chosen to be $n = 100$, i.e., each location was measured once with 100 transmit signals coherently integrated. The total RMSE error is 1.74 cm, which is the accuracy for a measurement distance from 80 cm to 280 cm. The fitting line in Figure 11 describes the regression line of the estimated distances. Hence, we can state that the system performs in the expected error ranges under very low multipath conditions.
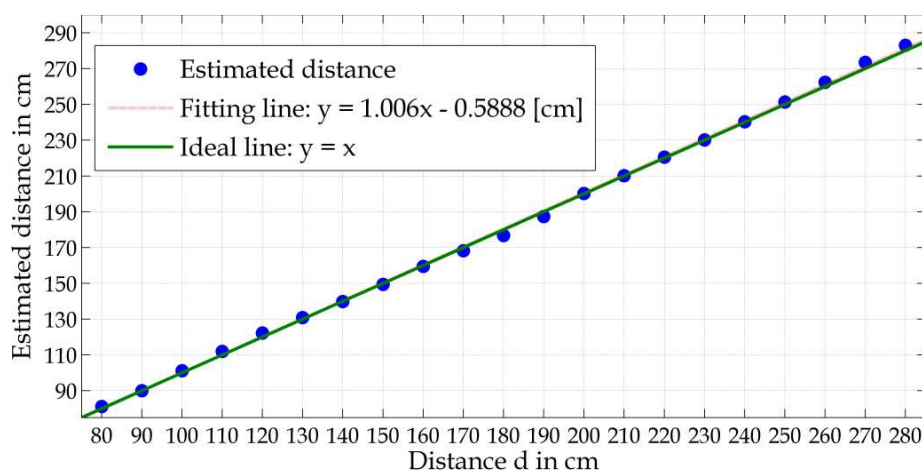

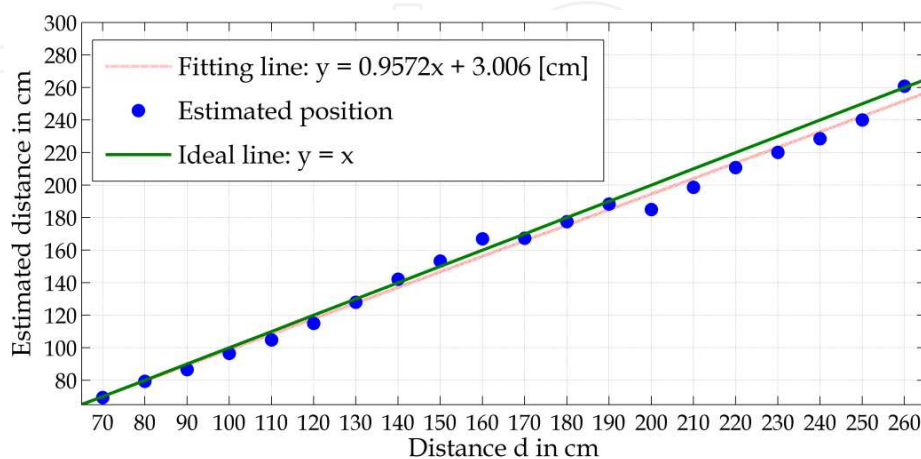**Figure 11.** Results of the measurement carried out in anechoic chamber

Figure 12. Results of the measurement carried out in an office environment

5.3. Office measurements

The results of the measurement carried out in the office environment are shown in Figure 12. Again, the x-axis describes the real distances between the antennas, the y-axis describes the estimated distances. The system is normalized to the distance of $d = 90$ cm, performed in the anechoic chamber. The coherent integration factor was chosen to be $n = 100$. The total RMSE error is 6.82 cm, which is the accuracy for a measurement distance from 70 cm to 260 cm. The fitting line describes the regression line of the estimated distances. The estimated values describe a nearly linear relation from 70 cm to 190 cm. The following estimated values are around 10 cm below the ideal line, the estimated value at the distance of 260 cm is back on track regarding the ideal line.

6. Result and discussion

The above measurements show that it is basically possible to gain range information down to accuracies of a few centimeters from the different modulation states of UHF RFID tags using wideband signals. However, there exist some simplifications, including the high-gain antennas and the tag modulation impedances given with open and short circuit (see also Subsection 5.2).

The idea behind the introduced localization system is based on the fact that current RFID-based localization systems either need a high effort in pre-calibration phases, suffer from bandwidth limitations, particularly in small frequency bands, e.g., as in Europe or need more complex hardware structures (phased array antennas) that only may be used in stationary, immobile applications. Therefore, a passive RFID-based positioning system should have ideally (Section 3) no change in hardware, high bandwidth, no pre-calibration phases and should be used in mobile applications. The suggested system includes these issues in the following way. There is no pre-calibration phase necessary as the system uses direct range estimation. This, however, is only possible due to the high bandwidth used along with low-power signals to stay within the required power spectrum densities. Changes in hardware would incorporate high bandwidth filter structures, a fast signal generator for the transmit pulses and a high accurate A/D converter for the incoming signals. Finally, it can be stated that such a localization system for mobile indoor positioning is possible, if the required hardware prerequisites are created.

7. Summary and conclusion

This chapter dealt with the concepts of localization comprising primarily UHF and microwave RFID systems. After describing the fundamental principles behind localization, a survey was given for state-of-the-art RFID localization systems. Subsequently, a novel RFID localization system using wideband signals was introduced. A theoretical derivation of the range deter-mination was given in Section 4, whereas Section 5 revealed the limits and challenges of the proposed localization system, e.g., through evaluation of the Cramér-Rao lower bound.

Finally, measurement results carried out in different environments (anechoic chamber, office) showed that the proposed system works within the former deduced limitations. The measurements showed a one-dimensional accuracy (RMSE) of 1.7 cm in the anechoic chamber, and an accuracy (RMSE) of 6.8 cm within the office environment. Tag reflection normalization and the usage of omni-directional antennas along with real-time localization are subjects to future work.

Acknowledgements

Author details

Andreas Loeffler[1*] and Heinz Gerhaeuser[2]

*Address all correspondence to: loeffler@like.eei.uni-erlangen.de

1 Chair of Information Technology (Communication Electronics) Engineering, Friedrich-Alexander-University of Erlangen-Nuremberg, Erlangen, Germany

2 Fraunhofer Institute for Integrated Circuits IIS, Erlangen, Germany

References

[1] Kaplan, E. D, & Hegarty, C. J. Understanding GPS: Principles And Applications. Artech House Mobile Communications Series. Artech House; (2006).

[2] Retscher, G, & Kealy, A. . Ubiquitous Positioning Technologies for Modern Intelligent Navigation Systems. The Journal of Navigation. (2006). ; . Available from: http://dx.doi.org/10.1017/S0373463305003504., 59(01), 91-103.

[3] Chen, Z, Xia, F, Huang, T, Bu, F, & Wang, H. . A localization method for the Internet of Things. The Journal of Supercomputing. (2011). ; . 10.1007/s11227-011-0693-2. Available from: http://dx.doi.org/10.1007/s11227-011-0693-2., 1-18.

[4] Xiang, Z, Song, S, Chen, J, Wang, H, Huang, J, & Gao, X. A wireless LAN-based indoor positioning technology. IBM Journal of Research and Development. (2004). sep;48(5.6): 617-626.

[5] Mautz, R. . Overview of current indoor positioning systems. Geodezija ir Kartografija. (2009). ; . Available from: http://www.tandfonline.com/doi/abs/10.3846/1392-1541.2009.35.18-22., 35(1), 18-22.

[6] Ashton, K. . Whither the Five-Cent Tag? RFID Journal; (2011). . Available from: http://www.rfidjournal.com/article/view/8212.

[7] Escribano, J. G, Garcia, A, Wissendheit, U, Loeffler, A, & Pastor, J. M. Analysis of the applicability of RFID & wireless sensors to manufacturing and distribution lines trough a testing multi-platform. In: Industrial Technology (ICIT), 2010 IEEE International Conference on; (2010). , 1379-1385.

[8] Baars, H, Gille, D, & Strüker, J. Evaluation of RFID applications for logistics: a frame-work for identifying, forecasting and assessing benefits. European Journal of Informa-tion Systems. (2009). , 18(6), 578-591.

[9] Desmons, D. . UHF Gen2 for item-level tagging. Presentation at RFID World. (2006). ;Available from: http://www.impinj.com/files/Impinj_ILT_RFID_WORLD.pdf.

[10] Dobkin, D. M. The RF in RFID: Passive UHF RFID in Practice. Communications Engineering Series. Elsevier / Newnes; (2007).

[11] Wackerly, D. D, Mendenhall, W, & Scheaffer, R. L. Mathematical Statistics with Applications. Thomson, Brooks/Cole; (2008).

[12] Manolakis, D. E. Efficient solution and performance analysis of 3-D position estimation by trilateration. Aerospace and Electronic Systems, IEEE Transactions on. (1996). oct;, 32(4), 1239-1248.

[13] Murphy, W. S. Determination of a Position Using Approximate Distances and Trilat-eration. Colorado School of Mines; (2007).

[14] Navidi, W. , Jr WSM, Hereman W. Statistical methods in surveying by trilateration. Computational Statistics & Data Analysis. (1998). ; . Available from: http://www.sciencedirect.com/science/article/pii/S0167947397000534., 27(2), 209-227.

[15] Hoene, C, & Willmann, J. Four-way TOA and software-based trilateration of IEEE 802.11 devices. In: Personal, Indoor and Mobile Radio Communications, 2008. PIMRC 2008. IEEE 19th International Symposium on; (2008). , 1-6.

[16] Arnitz, D, Muehlmann, U, Semiconductors, N, & Witrisal, K. Tag-Based Sensing and Positioning in Passive UHF RFID: Tag Reflection. In: 3rd Int. EURASIP workshop on RFID Technology; (2010).

[17] Liu, H, Darabi, H, Banerjee, P, & Liu, J. Survey of Wireless Indoor Positioning Techni-ques and Systems. Systems, Man, and Cybernetics, Part C: Applications and Reviews, IEEE Transactions on. (2007). nov;, 37(6), 1067-1080.

[18] Honkavirta, V, Perala, T, Ali-loytty, S, & Piche, R. A comparative survey of WLAN location fingerprinting methods. In: Positioning, Navigation and Communication, 2009. WPNC 2009. 6th Workshop on; (2009). , 243-251.

[19] Seitz, J, Vaupel, T, Jahn, J, Meyer, S, Boronat, JG, & Thielecke, J. . A Hidden Markov Model for urban navigation based on fingerprinting and pedestrian dead reckoning. In: Information Fusion (FUSION), 2010 13th Conference on; (2010). . . Available from: http://ieeexplore.ieee.org/stamp/stamp.jsp?tp=&arnumber=5712025., 1-8.

[20] Meyer, S. Feldstärkemessung; (2011).

[21] Nikitin, P. V, Martinez, R, Ramamurthy, S, Leland, H, & Spiess, G. Rao KVS. Phase based spatial identification of UHF RFID tags. In: RFID, 2010 IEEE International Conference on; (2010). , 102-109.

[22] Sanpechuda, T, & Kovavisaruch, L. A review of RFID localization: Applications and techniques. In: Electrical Engineering/Electronics, Computer, Telecommunications and Information Technology, 2008. ECTI-CON 2008. 5th International Conference on. (2008). , 2, 769-772.

[23] Zhang, Y, Li, X, & Amin, M. . In: Principles and Techniques of RFID Positioning. John Wiley & Sons, Ltd; (2010). . . Available from: http://dx.doi.org/ 10.1002/9780470665251.ch15., 389-415.

[24] Vossiek, M, Miesen, R, Wittwer, J, & Identification, R. F. and localization- recent steps towards the internet of things in metal production and processing. In: Microwave Radar and Wireless Communications (MIKON), 2010 18th International Conference on; (2010). , 1-8.

[25] Hightower, J, Want, R, & Borriello, G. SpotON: An indoor 3D location sensing technology based on RF signal strength. UW CSE 00-02-02, University of Washington, Department of Computer Science and Engineering, Seattle, WA. (2000). Available from: ftp://128.95.1.178/tr/2000/02/UW-CSE-00-02-02.pdf.

[26] Seidel, S. Y, & Rappaport, T. S. MHz path loss prediction models for indoor wireless communications in multifloored buildings. Antennas and Propagation, IEEE Transactions on. (1992). feb;, 40(2), 207-217.

[27] Bechteler, T. F, & Yenigun, H. D localization and identification based on SAW ID-tags at 2.5 GHz. Microwave Theory and Techniques, IEEE Transactions on. (2003). may;, 51(5), 1584-1590.

[28] Stelzer, A, Pourvoyeur, K, & Fischer, A. Concept and application of LPM- a novel 3-D local position measurement system. Microwave Theory and Techniques, IEEE Transactions on. (2004). dec;, 52(12), 2664-2669.

[29] Stove, A. G. Linear FMCW radar techniques. Radar and Signal Processing, IEE Proceedings F. (1992). oct;, 139(5), 343-350.

[30] Vossiek, M, Roskosch, R, & Heide, P. Precise 3-D Object Position Tracking using FMCW Radar. In: Microwave Conference, 1999. 29th European. (1999). , 1, 234-237.

[31] Heidrich, J, Brenk, D, Essel, J, Fischer, G, Weigel, R, & Schwarzer, S. Local positioning with passive UHF RFID transponders. In: Wireless Sensing, Local Positioning, and

RFID, 2009. IMWS 2009. IEEE MTT-S International Microwave Workshop on; (2009). , 1-4.

[32] Li, X, Zhang, Y, & Amin, M. G. Multifrequency-based range estimation of RFID Tags. In: RFID, 2009 IEEE International Conference on; (2009). , 147-154.

[33] Ni, L. M, Liu, Y, Lau, Y. C, & Patil, A. P. LANDMARC: indoor location sensing using active RFID. Wireless networks. (2004). , 10(6), 701-710.

[34] Hightower, J, Vakili, C, Borriello, G, & Want, R. Design and calibration of the spoton ad-hoc location sensing system. unpublished, August. (2001).

[35] Chattopadhyay, A, & Harish, A. R. Analysis of low range Indoor Location Tracking techniques using Passive UHF RFID tags. In: Radio and Wireless Symposium, 2008 IEEE. IEEE; (2008). , 351-354.

[36] Chattopadhyay, A, & Harish, A. R. Analysis of UHF passive RFID tag behavior and study of their applications in low range indoor location tracking. In: Antennas and Propagation Society International Symposium, 2007 IEEE; (2007). , 1217-1220.

[37] Park, S, & Lee, H. Self-recognition of Vehicle Position using UHF Passive RFID Tags. (2012).

[38] Hahnel, D, Burgard, W, Fox, D, Fishkin, K, & Philipose, M. Mapping and localization with RFID technology. In: Robotics and Automation, 2004. Proceedings. ICRA'04. 2004 IEEE International Conference on. IEEE; (2004). , 1, 1015-1020.

[39] Hahnel, D, Burgard, W, Fox, D, & Thrun, S. An efficient fastSLAM algorithm for generating maps of large-scale cyclic environments from raw laser range measurements. In: Intelligent Robots and Systems, 2003. (IROS 2003). Proceedings. 2003 IEEE/RSJ International Conference on. (2003). vol.1., 1, 206-211.

[40] Dellaert, F, Fox, D, Burgard, W, & Thrun, S. Monte Carlo localization for mobile robots. In: Robotics and Automation, 1999. Proceedings. 1999 IEEE International Conference on. (1999). vol.2., 2, 1322-1328.

[41] Parlak, S, & Marsic, I. Non-intrusive localization of passive RFID tagged objects in an indoor workplace. In: Proc. IEEE Int RFID-Technologies and Applications (RFID-TA) Conf; (2011). , 181-187.

[42] Friedman, J, Hastie, T, & Tibshirani, R. Additive logistic regression: a statistical view of boosting (With discussion and a rejoinder by the authors). The annals of statistics. (2000). , 28(2), 337-407.

[43] Karmakar, N. C, Roy, S. M, & Ikram, M. S. Development of Smart Antenna for RFID Reader. In: RFID, 2008 IEEE International Conference on; (2008). , 65-73.

[44] Finkenzeller, K. RFID Handbook: Fundamentals and Applications in Contactless Smart Cards, Radio Frequency Identification and Near-Field Communication. Wiley; (2010).

[45] Taylor, J. D. Introduction to ultra-wideband radar systems. CRC; (1995).

[46] Loeffler, A, & Gerhaeuser, H. A Novel Approach for UHF-RFID-Based Positioning Through Spread- Spectrum Techniques. Smart Objects: Systems, Technologies and Applications (RFID Sys Tech), 2010 European Workshop on. (2010). june;, 1-10.

[47] Ussmueller, T, Brenk, D, Essel, J, Heidrich, J, Fischer, G, & Weigel, R. A multistandard HF/ UHF-RFID-tag with integrated sensor interface and localization capability. In: RFID (RFID), 2012 IEEE International Conference on; (2012). , 66-73.

[48] Loeffler, A. Localizing passive UHF RFID tags with wideband signals. In: Microwaves, Communications, Antennas and Electronics Systems (COMCAS), 2011 IEEE International Conference on; (2011). , 1-6.

[49] Gustafsson, F, & Gunnarsson, F. Mobile positioning using wireless networks: possibilities and fundamental limitations based on available wireless network measurements. Signal Processing Magazine, IEEE. (2005). july;, 22(4), 41-53.

[50] Fowler, M. . EECE 522 Estimation Theory; (2012). . Available from: http://www.ws.binghamton.edu/fowler/fowler%20personal%20page/EE522.htm.

[51] Gezici, S. . A Survey on Wireless Position Estimation. Wireless Personal Communications. (2008). ; . 10.1007/s11277-007-9375-z. Available from: http://dx.doi.org/10.1007/s11277-007-9375-z., 44, 263-282.

[52] Arnitz, D, Adamiuk, G, Muehlmann, U, & Witrisal, K. . UWB channel sounding for ranging and positioning in passive UHF RFID. 11th COST2100 MCM. (2010). ;Available from: http://spsc.tu-graz.ac.at/system/files/arnitzcostmcm10.pdf.

[53] Arnitz, D, Muehlmann, U, & Witrisal, K. UWB ranging in passive UHF RFID: proof of concept. Electronics Letters. (2010). , 46(20), 1401-1402.

[54] Viikari, V, Pursula, P, & Jaakkola, K. Ranging of UHF RFID Tag Using Stepped Frequency Read-Out. Sensors Journal, IEEE. (2010). sept;, 10(9), 1535-1539.

[55] Loeffler, A. Dispersion Effects at High Bandwidth Localization for UHF RFID Tags. ITG-Fachbericht-Smart SysTech 2012. (2012).